Calculation of Magnetic Field from a Current Carrying Finite Size Conductor

T.F. Yang

June 1973

UWFDM-47

FUSION TECHNOLOGY INSTITUTE

UNIVERSITY OF WISCONSIN

MADISON WISCONSIN

Calculation of Magnetic Field from a Current Carrying Finite Size Conductor

T.F. Yang

Fusion Technology Institute
University of Wisconsin
1500 Engineering Drive
Madison, WI 53706

http://fti.neep.wisc.edu

June 1973

UWFDM-47

CALCULATION OF MAGNETIC FIELD FROM A CURRENT CARRYING FINITE SIZE CONDUCTOR

by

T. F. Yang

June 1973

FDM 47

University of Wisconsin

ABSTRACT

A computer code MAFCO-W has been written for calculating magnetic fields of finite size conductors of any configuration which can be approximated by arc segments or straight segments of rectangular cross section. The magnetic field components were obtained by integrating the Biot-Savat's law over the volume of the conductor. Their mathematic expressions were first reduced to single integration analytically and then integrated numerically.

I. Introduction

Stress analysis for a large magnetic coil, such as the constant tension D-shaped magnetic used in Tokamak reactors, requires accurate knowledge of the magnetic field inside the coil. The general program MAFCO handles only the case for filament windings and can lead to difficulties inside the conductor. Therefore, a new code has been written to calculate the field necessary for the stress analysis.

To calculate the field from a solid conductor, one has to integrate the three dimensional field components given by Biot-Savat's law over the volume of the conductor. Thus, three dimensional integrations were involved. It is impractical and often too time consuming to carry out the triple integrations straight forward numerically. In this report, the expressions for the field components were reduced to single integration for a straight segment in Cartesian coordinates and for an arc segment in cylindrical coordinates. Some exact solutions were also obtained. The final results were evaluated numerically. Using the transformation method given in MAFCO, the field at any point in space and the continuation of field line passing through any desired point in space can be calculated from any current carrying conductor of arbitrary geometry. A Wisconsin version MAFCO-W was written to accomplish this purpose.*

II. Theory

A. The field from a circular arc segment and ring is shown by Figure 1. The magnetic field at the point p(Rp, θp, Zp) from a source

---

* Final report is in progress.

element dl at the point (ρ, ϕ, Z) is given by the Biot-Savat's law:

$$d\vec{B}_p = \frac{j\, d\vec{l} \times \vec{R}\, d\rho\, dZ}{10\, R^3} \tag{1}$$

where j is the current density in amp/cm^2 and $\vec{R}$ is the position vector from $\vec{dl}$ to p which is

$$R^2 = R_p^2 - 2R_p\, \rho \cos(\phi_p - \phi) + \rho^2 + (Z_p - Z)^2 \tag{2}$$

Letting $\theta = \phi - \phi_p$

$$\begin{aligned} dl &= \hat{R}_p \cdot \rho d\phi \sin\theta + R_p\, \hat{\phi}_p \cdot \rho d\phi \cos\theta + \hat{Z}_p \cdot 0, \\ \text{and}\quad \vec{R} &= \hat{R}_p \cdot (R_p - \rho\cos\theta) + R_p\, \hat{\phi}\ (\rho \sin\theta) + \hat{Z}(Z_p - Z). \end{aligned} \tag{3}$$

The vector product of $\vec{R}$ and $\vec{dl}$ is

$$\vec{R} \times \vec{dl} = \begin{vmatrix} \hat{R}_p & R_p\, \hat{\phi}_p & \hat{Z}_p \\ R_p - \rho\cos\theta & \rho\sin\theta & Z_p - Z \\ \rho d\phi \sin\theta & \rho d\phi \cos\theta & 0 \end{vmatrix},$$

$$= \hat{R}_p\, [\rho(Z_p - Z)\cos\theta\, d\phi] + R_p\, \hat{\phi}_p\, (Z_p - Z)\, \rho \sin\theta\, d\phi$$

$$+ \hat{Z}(\rho^2 - R_p\, \rho\cos\theta) d\phi. \tag{4}$$

Thus the components of $d\vec{B}_p$ are

$$dB_{R_P} = \frac{j(Z_p - Z)\rho\cos\theta\, dZ\, d\rho\, d\theta}{10[\rho^2 - 2\rho\, R_p \cos\theta + R_p^2 + (Z_p - Z)^2]^{3/2}}, \tag{5}$$

$$dB_{\phi_P} = \frac{j(Z_p - Z)\rho\sin\theta\, dZ\, d\rho\, d\theta}{10[\rho^2 - 2\rho\, R_p \cos\theta + R_p^2 + (Z_p - Z)^2]^{3/2}}, \tag{6}$$

$$\text{and} \quad dH_{z_p} = \frac{j(\rho^2 - \rho R_p \cos\theta)dZ\, d\rho\, d\theta}{10[\rho^2 - 2\rho R_p \cos\theta + R_p^2 + (Z_p - Z)^2]^{3/2}}. \qquad (7)$$

In the following discussions, the integration limits are from θ_1 to θ_2, Z_1 to Z_2 and ρ_1 to ρ_2, unless otherwise specified, for a ciruclar arc of rectangular cross-section. B_θ can be obtained exactly if we integrate equation (6) over θ and Z successively, thus

$$B_{\phi_p} = \frac{j}{10} \int d\rho \int dZ \frac{(Z_p - Z)dZ}{R_p[\rho^2 - 2R_p \rho \cos\theta + R_p^2 + (Z_p - Z)^2]^{3/2}} + C,$$

$$= -\frac{j}{10} \int \frac{1}{R} [\rho^2 - 2R_p \rho \cos\theta + R_p^2 + (Z_p - Z)^2]^{1/2} d\rho + C.$$

This can be rewritten as

$$B_{\phi_p} = -\frac{j}{10 R_p} \int [(\rho - R_p \cos\theta)^2 + R_p^2 \sin^2\theta + (Z_p - Z)^2]^{1/2} d\rho + C,$$

integrating we obtain

$$B_{\phi_p} = -\frac{j}{20 R_p} \{(\rho - R_p \cos\theta)R_p + [R_p^2 + \sin^2\theta + (Z_p - Z)^2] \cdot \log[(\rho - R_p \cos\theta)R]\} + C. \qquad (8)$$

For the components B_ρ and B_Z the integrations over Z and ρ can be carried out. From equations (6) and (7) and according to T. H. Boyer et. al.[2] and E. C. Paxhia[2] they are given as follows:

$$B_{R_p} = \frac{j}{10} \int d\theta \cos\theta \{R + R_p \cos\theta \log(\rho - R_p \cos\theta + R)\} + C, \quad (9)$$

$$\text{and} \quad B_{Z_p} = \frac{j}{10} \int d\theta (Z - Z_p)\{\log(\rho - R_p\cos\theta + R) + \frac{R_p \cos\theta}{2|Z_p - Z|} \log \frac{R - |Z_p - Z|}{R + |Z_p - Z|} - \frac{R_p |\sin\theta|}{|Z_p - Z|} \tan^{-1}\left[\frac{(\rho - R_p\cos\theta)|Z_p - Z|}{R_p |\sin\theta| R}\right] + C. \qquad (10)$$

If the field point is on the Z-axis, B_ρ, B_ϕ and B_Z become

$$B_{R_p} = \frac{j}{10}(Z - Z_p)\log(\rho + \sqrt{\rho^2 + (Z_p - Z)^2}) + C,$$

$$B_{\phi_P} = \frac{j}{10\,R_p}\cos\theta[\rho^2 + (Z_p - Z)^2]^{1/2} + C, \tag{11}$$

and $$B_{Z_P} = \frac{j}{10}(Z - Z_p)\log\left\{\frac{R + [R^2 + (Z_p - Z)^2]^{1/2}}{R + [R^2 + (Z_p - Z)^2]^{1/2}}\right\} + C.$$

In the case of circular ring of rectangular cross section, the expression for B_ρ, B_ϕ and B_Z are the same as equations (8), (9), (10) and (11), but the integration limits over θ is from 0 to 2π. Due to the symmetry property of B_ρ and B_Z, we can just integrate them from 0 to π and multiply the results by 2. It follows that B_ϕ is zero everywhere and B_ρ is zero on the z-axis.

It would be useful to obtain the expressions for a thin arc sheet, i.e. when $Z_2 \approx Z_1 = Z_0$. From equation (4), the component B_ϕ is then

$$B_{\phi_P} = \frac{j}{10}(Z_p - Z_0)\int d\rho \int d\phi \frac{\rho\sin\theta}{[\rho^2 - 2\rho R_p\cos\theta + R_p^2 + (Z_p - Z_0)]^{3/2}},$$

integrating over θ and rewriting the denominator

$$B_{\phi_P} = \frac{j}{10}\frac{(Z_p - Z_0)}{R_p}\int d\rho \frac{1}{[(\rho^2 - R_p\cos\theta)^2 + R_p^2\sin^2\theta + (Z_p - Z_0)^2]^{1/2}},$$

$$= \frac{j}{10}\frac{(Z_p - Z_0)}{R_p}\log[\rho - R_p\cos\theta + R]. \tag{12}$$

Here j is amp/cm and $R^2 = \rho^2 - 2\rho R_p \cos\theta + R_p^2 + (Z_p - Z_0)^2$. After rewriting the denominator from equation (3)

$$B_{R_P} = \frac{j}{10} \int d\theta \int d\rho \frac{\rho \cos\theta}{[(\rho^2 - R_p \cos\theta)^2 + R_p^2 \sin^2\theta + (Z_p - Z_0)^2]^{3/2}},$$

$$= \frac{j}{10} R_p \int d\theta \{\cos^2\theta \log[\rho - R_p \cos\theta + \sqrt{\rho^2 - 2\rho R_p \cos\theta + R_p^2 + (Z_p - Z_0)^2}]$$

$$- \cos\theta [\rho^2 - 2\rho R_p \cos\theta + R_p^2 + (Z_p - Z_0)^2]^{-1/2}\}$$

By letting $\theta = \pi + 2\phi - \theta_1$ and $k^2 = 4\rho R_p[(\rho + R_p)^2 + (Z_p - Z_0)^2]^{-1}$ the second term can be transferred into the sum of incomplete elliptic integrals of first kind and second kind.[3]

$$E(k,W) = \int_0^W (1 - k^2 \sin^2\phi)^{-1/2} d\phi,$$

and

$$K(k,W) = \int_0^W (1 - k^2 \sin^2\phi)^{1/2} d\phi.$$

when $W = (\theta_2 - \theta_1)/2$. Then we can write

$$B_\rho = \frac{j}{10} R_p \int d\theta \{\cos^2\theta \log[\rho - R_p \cos\theta + R]\}$$

$$+ \frac{j}{10} (\rho R_p)^{1/2}[(1 - 1/2k^2)K - E]. \qquad (13)$$

From equation (7)

$$B_{Z_P} = \frac{j}{10} \int d\theta \int d\rho \frac{\rho(\rho - R_p \cos\theta)}{[(\rho - R_p \cos\theta)^2 + R_p^2 \sin\theta + (Z_p - Z_o)^2]^{3/2}},$$

Integrating by parts

$$B_{Z_P} = \frac{j}{10}\left[\int \frac{\rho d\theta}{[\rho^2 - 2\rho R_p \cos\theta + R_p^2 + (Z_p - Z_o)^2]^{1/2}} + \int \frac{d\rho\, d\theta}{[(\rho - R_p\cos\theta)^2 + R_p^2\sin^2\theta + (Z_p - Z_o)^2]^{3/2}}\right] + C.$$

The first term can also be transformed into elliptic integrals and the second term can be integrated over ρ as usual, then

$$B_{Z_P} = \frac{j}{10}\{\frac{2}{\sqrt{(\rho - R_p)^2 + (Z_p - Z_o)^2}} E(k,w) + \int \log[\rho - R_p\cos\theta + R]d\theta\}. \quad (14)$$

(A.) Field From a Straight Segment of Rectangualr Cross Section

If we transform any arbitrarily oriented current carrying straight segment of conductor to a coordinate such that the current flows in the Z-direction as shown by Figure 2, then the field at the point $p(X_p, X_p, Z_p)$ due to a current element $\vec{dz}$ at the source point (x, y, z) is

$$\vec{dH} = \frac{j\, dx\, dy}{10\, R^3}(\vec{dz} \times \vec{B}),$$

$$= \frac{j\,\rho}{10\, R^3}\ \hat{z} \times \hat{R}\, dx\, dy\, dz, \quad (15)$$

where $\rho = \sqrt{(Z_p - x)^2 + (Y_p - y)^2}$

and $R = \sqrt{(Z_p - x)^2 + (Y_p - Y)^2 + (Z_p - Z)^2}$

The x and y components of $\vec{dB}$ are

$$dB_{x_P} = -\frac{j}{10}\frac{Y_p - Y}{R^3}\,dx\,dy\,dZ, \tag{16}$$

and

$$dB_{y_P} = +\frac{j}{10}\frac{X_p - X}{R^3}\,dx\,dy\,dZ. \tag{17}$$

After carrying out the integration of Z in equation (16)

$$B_{x_P} = \int\int -\frac{j}{10}\,\frac{(Y_p - Y)(Z_p - Z)\,dxdy}{[(X_p - X)^2 + (Y_p - Y)^2]\sqrt{(X_p - X)^2 + (Y_p - Y)^2 + (Z_p - Z)^2}} + C. \tag{18}$$

Making the substitution $t^2 = (X_p - X)^2 + (Y_p - Y)^2 + (Z_p - Z)^2$ we can integrate out Y and obtain

$$B_{x_P} = -\frac{j}{20}\int dx\,\frac{(Z_p - Z)}{|Z_p - Z|}\,\log\frac{R - |Z_p - Z|}{R + |Z_p - Z|} + C. \tag{19}$$

Similarly the y-component of B is

$$B_{y_P} = -\frac{j}{10}\int dy\,\frac{(Z_p - Z)}{|Z_p - Z|}\,\log\frac{R - |Z_p - Z|}{R + |Z_p - Z|} + C. \tag{20}$$

Equations (18) and (19) consist of single integration which will be integrated numerically.

In case of a thin rectangular sheet of finite length, e.g. $y_1 \tilde{} y_2 = y_0$, equation (18) is reduced to single integration

$$B_{x_P} = -\frac{j}{10}\int \frac{(Y_p - Y_o)(Z_p - Z)dx}{[(X_p - X)^2 + (Y_p - Y)^2]\sqrt{(X_p - X)^2 + (Y_p - Y)^2 + (Z_p - Z)^2}} + C. \tag{21}$$

which can be integrated after making the substitution

$$\sqrt{(X_p - X)^2 + (Y_p - Y_o)^2} = |Z_p - Z| \tan\theta$$

then,

$$B_{x_p} = -\frac{j}{10} \frac{(Z_p - Z)(Y_p - Y_o)}{|Z_p - Z|} \left[\log \frac{R - |Z_p - Z|}{\sqrt{(X_p - X)^2 + (Y_p - Y_o)^2}} + \frac{R}{|Z_p - Z|} \right] + C. \tag{22}$$

The y-component is

$$B_{y_p} = -\frac{j}{10} \int \frac{(X_p - X)(Z_p - Z)dx}{\sqrt{(X_p - X) + (Y_p - Y)^2 + (Z_p - Z)^2}[(X_p - X)^2 + (Y_p - Y_o)^2]} + C,$$

$$= -\frac{j}{10} (Z_p - Z) \log \frac{\sqrt{(X_p - X)^2 + (Y_p - Y_o)^2} - |Z_p - Z|}{R + |Z_p - Z|} + C. \tag{23}$$

The integration limits are from X_1 to X_2 and Z_1 to Z_2 for both equations (19) and (20). Similarly expressions can be obtained for B_x and B_y when $X_1 \cong X_2 = X_o$. However, due to symmetry, this can be transformed to the case $Y_1 = Y_2 = Y_o$.

In the case of an infinitely long segment, after taking the limit $|Z_p - Z| \to \infty$ equation (17) becomes

$$B_{x_p} = -\frac{j}{10} \int \int \frac{(X_p - X)\, dxdy}{\sqrt{(X_p - X)^2 + (Y_p - Y)^2}} + C.$$

After integrating over y

$$B_{x_p} = -\frac{j}{10} \int \log [(X_p - X)^2 + (Y_p - Y)^2] dy + C.$$

which can be rewritten as

$$B_{x_p} = -\frac{j}{10}\int |X_p - X| \log\left(|X_p - X|^2 \sec^2\theta\right) d(\tan\theta).$$

With the change of variable $Y_p - Y = |X_p - X|\tan\theta$, and integrating by parts twice we obtain

$$B_{x_p} = -\frac{j}{10}|X_p - X|\left\{2\tan^{-1}\frac{Y_p - Y}{|X_p - X|} + \frac{Y_p - Y}{|X_p - X|}\left[\log\left[(X_p - X)^2+(Y_p-Y)^2\right]-2\right]\right\}. \tag{23}$$

Similarly an expression for B_y can be obtained by interchanging the role of x and y in equation (23).

III. The Considerations for Numerical Integration

In order to obtain reliable results and high computing efficiency of the numerical integration, the properties of the integrands of the expressions in the last two sections were examined. In the case of arc segment, the terms involved in the integrand in the expressions (8) to (11) can be classified into the forms:

$$f_1 = \log\left(\rho - R_p\cos\theta + \sqrt{\rho^2 - 2\rho R_p\cos\theta + R_p^2 + (Z_p - Z)^2}\right),$$

$$f_2 = R_p\cos\theta\log\frac{\sqrt{\rho 2 - 2\rho R_p\cos\theta + R_p^2 + |Z_p - Z|^2} - |Z_p - Z|^2}{\sqrt{\rho^2 - 2\rho R_p\cos\theta + R_p^2 + |Z_p - Z|^2} + |Z_p - Z|^2},$$

and $$f_3 = R_p|\sin\theta|\tan^{-1}\left[\frac{(\rho - R_p\cos\theta)|Z_p - Z|}{R_p|\sin\theta|\sqrt{\rho^2 - 2\rho R_p\cos\theta + R_p^2} + |Z_p - Z|^2}\right].$$

Except at the singular point $Z_p = Z$, $\rho = R_p$ and $\theta = 0$ the variation of f_1 can be shown by Figure 3. f_1 increases from large negative value at $\theta = 0$ and passes zero at some angle $\theta_o = \frac{\pi}{2}$. The argument of the logarithmic finction in f_2 is always less than 1 and so the value of the logarithmic function is always less than zero. Because f_2 is a product of $\cos\theta$ and logarithmic function, it varies like f_2 but with zero value at $\theta_o = \frac{\pi}{2}$.

The arctangent function in f_3 is varying from $-\pi$ to π when $\rho < R_p$ and varying between 0 and π when $\rho > R_p$, therefore, its product with $|\sin\theta|$ are shown by Figures 4a and 4b. One can use Simpson's rule with a large number of integration steps for all cases. However, for saving computation time and inproving accuracy, one can also choose Simpson's rule for the region $\theta = 0$ to θ_0 for f_1 and f_2 and use Gaussian Quadrature for the rest of the calculations.

In evaluating the integrands, expansions have to be made in the following cases.

(1) If $2\rho R_p(1 - \cos\theta) < 0.1\ (\rho - R_p)^2$ and $(\rho - r)<0$

$$\rho - R_p \cos\theta + \sqrt{\rho^2 - 2\rho R_p \cos\theta + R_p^2}$$

$$= R_p(1 - \cos\theta) + (\rho - R_p)\{1/2\ x^2 - 1/4 + 1/16\ x^3 - 5/128\ x^4 + \ldots\},$$

where $x = \dfrac{2\rho R_p(1 - \cos\theta)}{(\rho - R_p)2}$

(2) If $\rho - 2\rho R_p \cos\theta + R_p^2 \leq 0.01(Z_p - Z)^2$

$$\sqrt{\rho^2 - 2\rho R_p \cos\theta + R_p^2 + (Z_p - Z)^2} - |Z_p - Z|$$

$$= |Z_p - Z|^2[1/2\ x^2 - 1/4\ x^2 + 1/16\ x^3 - 5/128\ x^4 + \ldots]$$

In the case of straight segment, the integrands are smooth varying functions. The $\vec{dB}$ is zero at the singular point $R_p = \rho$ inside the conductor because jd x dy decrease as R^2 and approaches zero faster than the denominator. The integrands have also to be expanded in the following cases

(1) If $|Z_p - Z| > (X_p - X)^2 + (Y_p - Y)^2$

$$\sqrt{(X_p - X)^2 + (Y_p - Y)^2 + (Z_p - Z)^2} - |Z_p - Z|$$

$$= (Z_p - Z)[1/2\ u - 1/8u^2 + 1/16\ u^3 - 5/128\ u^4 + \ldots]$$

where $$u = \frac{(X_p - X)^2 + (Y_p - Y)^2}{(Z_p - Z)^2}$$

(2) If $X_p X < X_p^2 + X^2 + (Z_p - Z)^2 + (Y_p - Y)^2$,

then $$\log\{\sqrt{(X_p - X)^2 + (Y_p - Y)^2 + (Z_p - Z)^2} - |Z_p - Z|\},$$

$$= \log[R - |Z_p - Z|] + 1u\ [1 + \frac{R}{R - |Z_p - Z|}(-1/2w - 1/8w^2 - 1/16w^3 - 5/128w^4)],$$

$$= \log[R - |Z_p - Z|] + \upsilon - 1/2\ \upsilon^2 - 1/4\ \upsilon^4 + \ldots,$$

where $$W = \frac{X_p X}{X_p^2 + X^2 + (Z_p - Z)^2 + (Y_p - Y)^2},$$

$$\upsilon = \frac{R}{R - |Z_P - Z|} (-1/2w - 1/8w^2 - 1/16w^3 + \ldots).$$

Similarly expansions have to be made for

$$Y_P Y < Y_P^2 + Y^2 + (Z_P - Z)^2 + (X_P - X)^2,$$

or $$X_P X + Y_P Y < X_P^2 + X^2 + (Z_P - Z)^2 + Y_P^2 + Y^2.$$

V. Sample Problem

The magnetic field calculations for Wisconsin Tokamak (UWMACK) is presented here as an example. UWMAK has 12 constant tension D-shaped magnetic field coils spaced at equal angular interval of 30°. The upper half of each coil is shown in Fig. 5. Each half of the coil is approcimated by 6 arcs and one straight segment which is the minimum number of segments to give a smooth connection between each other. The dashed lines are the radius of curvatures. α_1 and α_2 are the integration limits for the second segment.

The calculated field pattern of the first guadrant along the torus on the midplane is presented in Fig. 6. The field pattern in the other three quadrant are the same due to periodicity of the coil arrangement. The cross-sections of the magnetic field coils are shown by the dashed rectangulars. The plasma occupies the space within the shaded field lines. Fig. 7 shows the magnitude of the field along the radii at 0° and 15° on midplane. The field variation along the field line on the outer edge of the plasma is shown by Fig. 8.

VII. References

1. W. A. Perkins and J. C. Brown, "MAFCO - A Magnetic Field Code for Handling General Current Elements in Three Dimensions," LRL Rept. UCRL - 7744 - Rev. II.

2. T. H. Boyler and G. L. Droyles, Electromagnetic Field Code, Oak Ridge National Laboratory Rept. Rough Draft and subsequently revised by Emmanuel C. Paxhia, Computor Program for the Magnetic Field of a Solenoid, McDonnell Research Division Rept. 9060.

3. W. R. Smythe, Static and Dynamic Electricity (McGraw-Hill Book Co., New York, 1950). 2nd ed., p. 271.

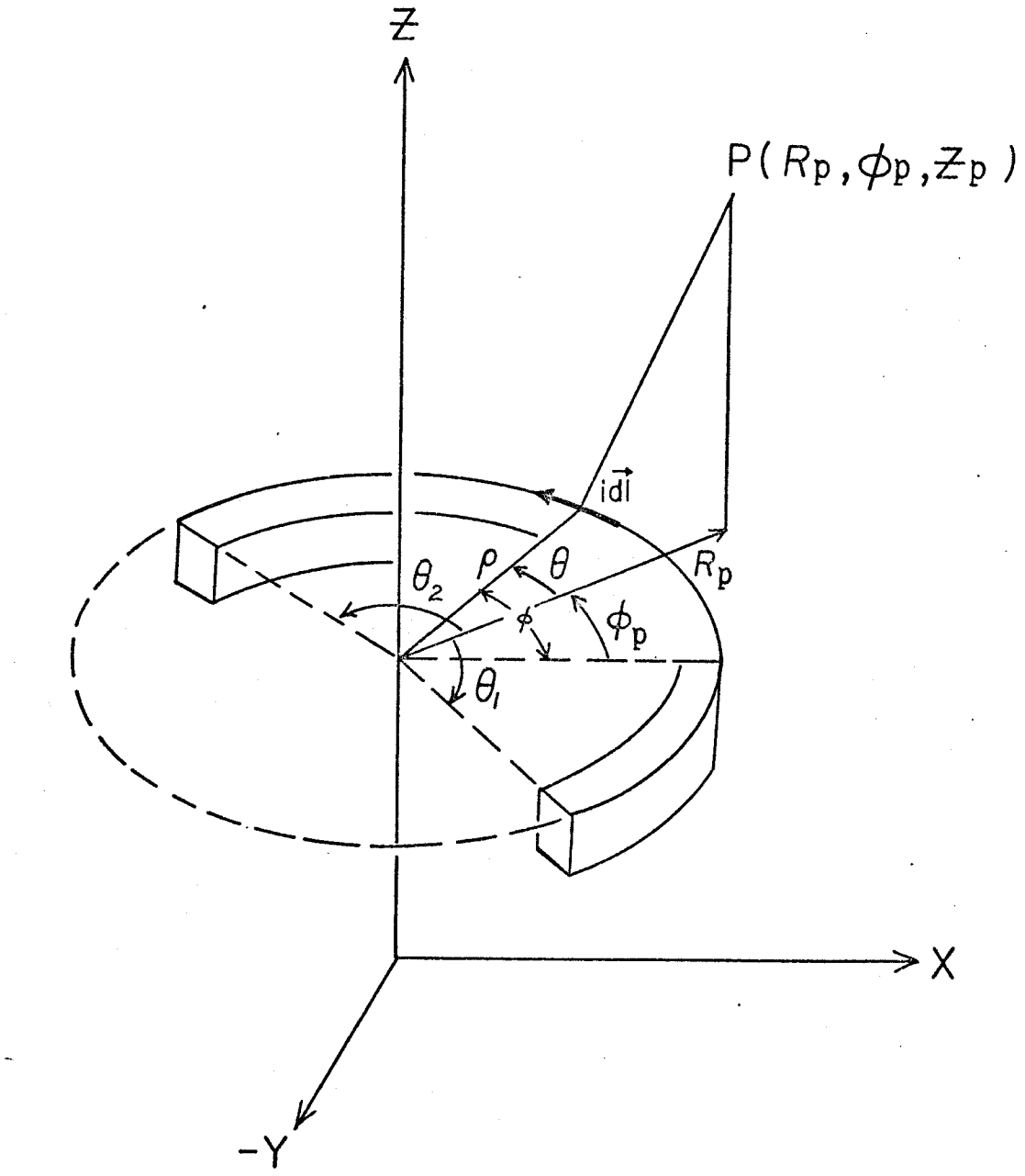

FIGURE 1 Arc Segment Coordinates

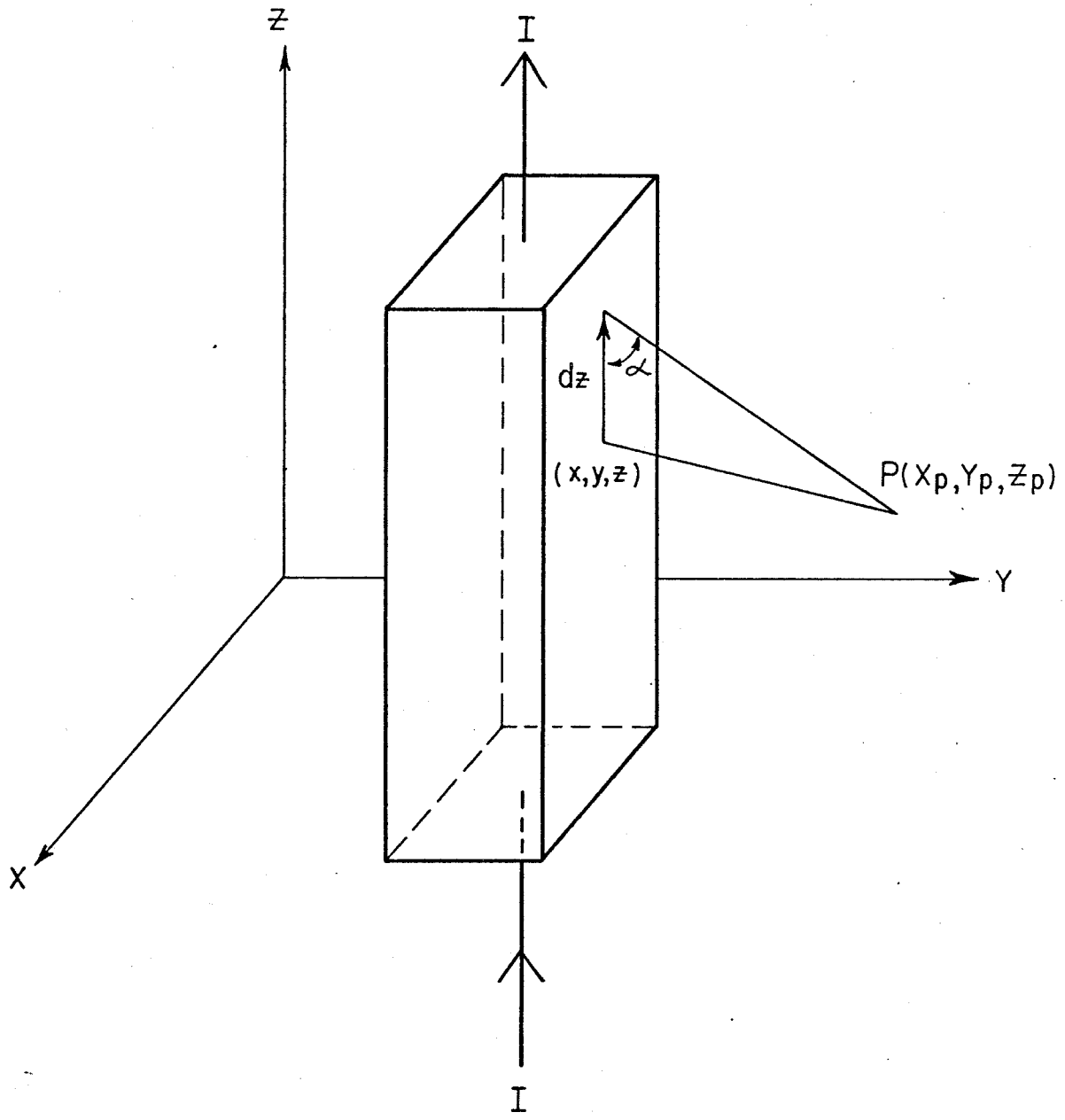

FIGURE 2 Straight Segment Field Components

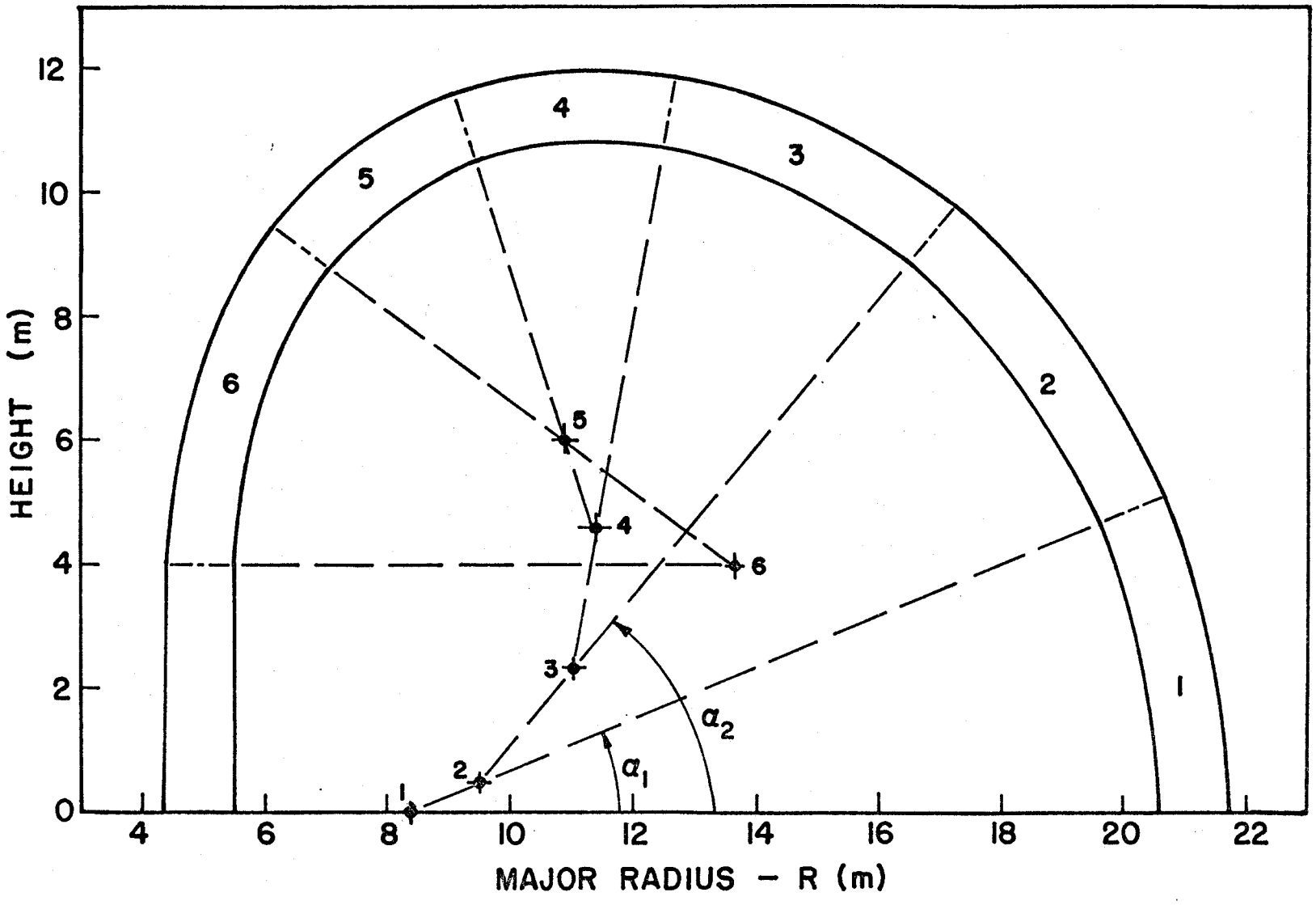

FIGURE 3 Geometry of Toroidal Magnetic Field Coil

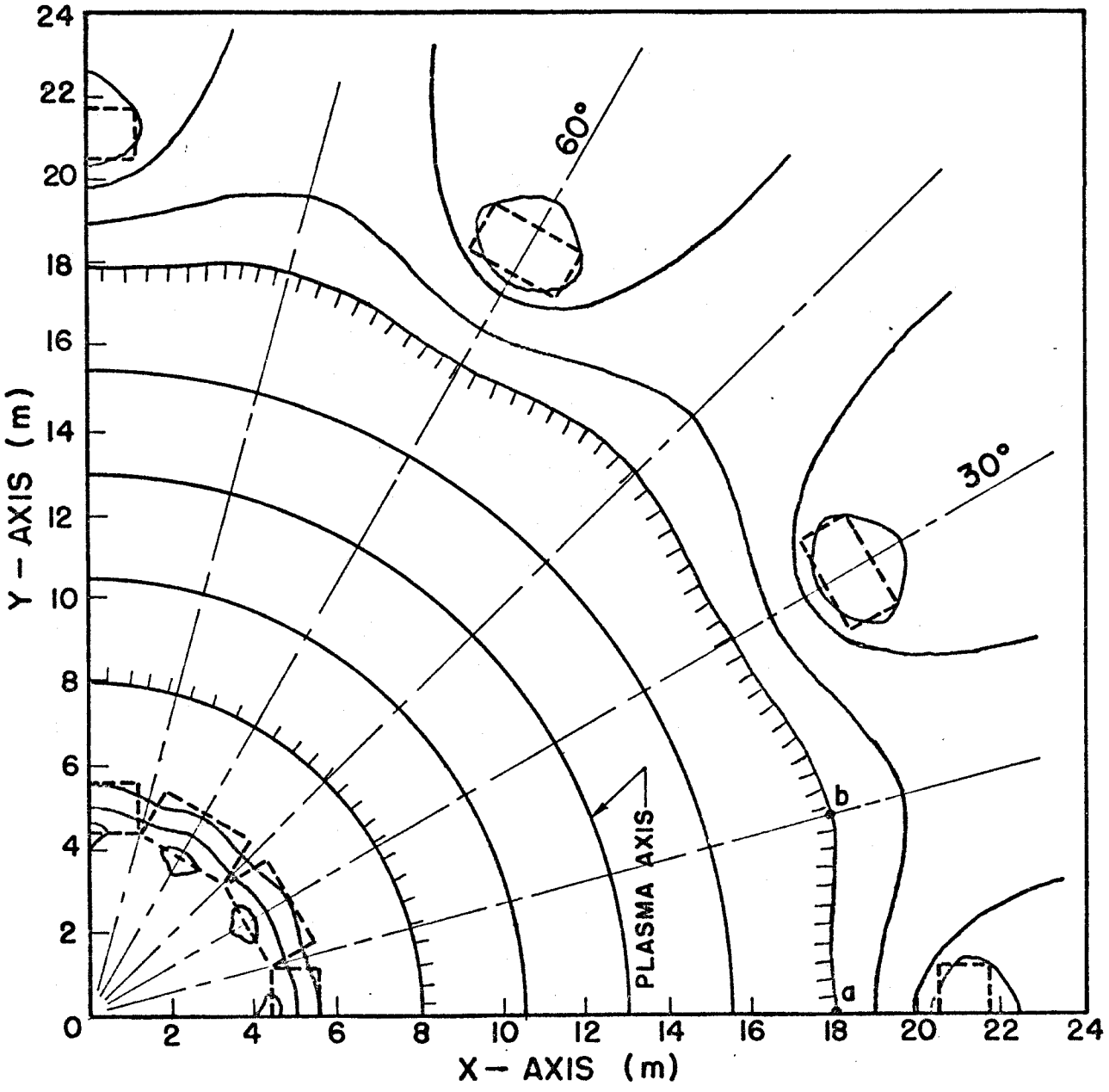

FIGURE 4 Field Pattern on Midplane of Torus

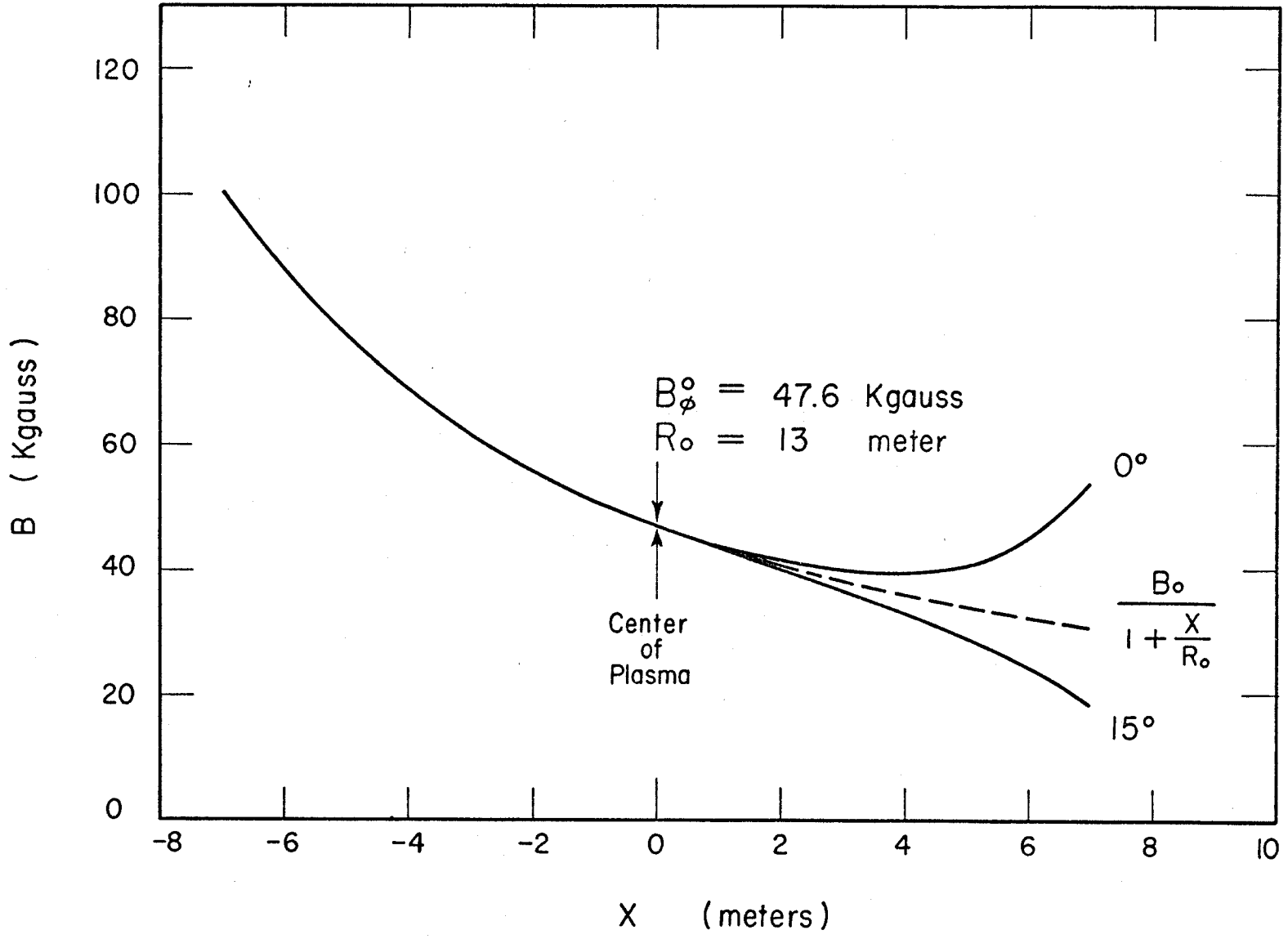

FIGURE 5
Field Magnitude Along Minor Radius at Midplane

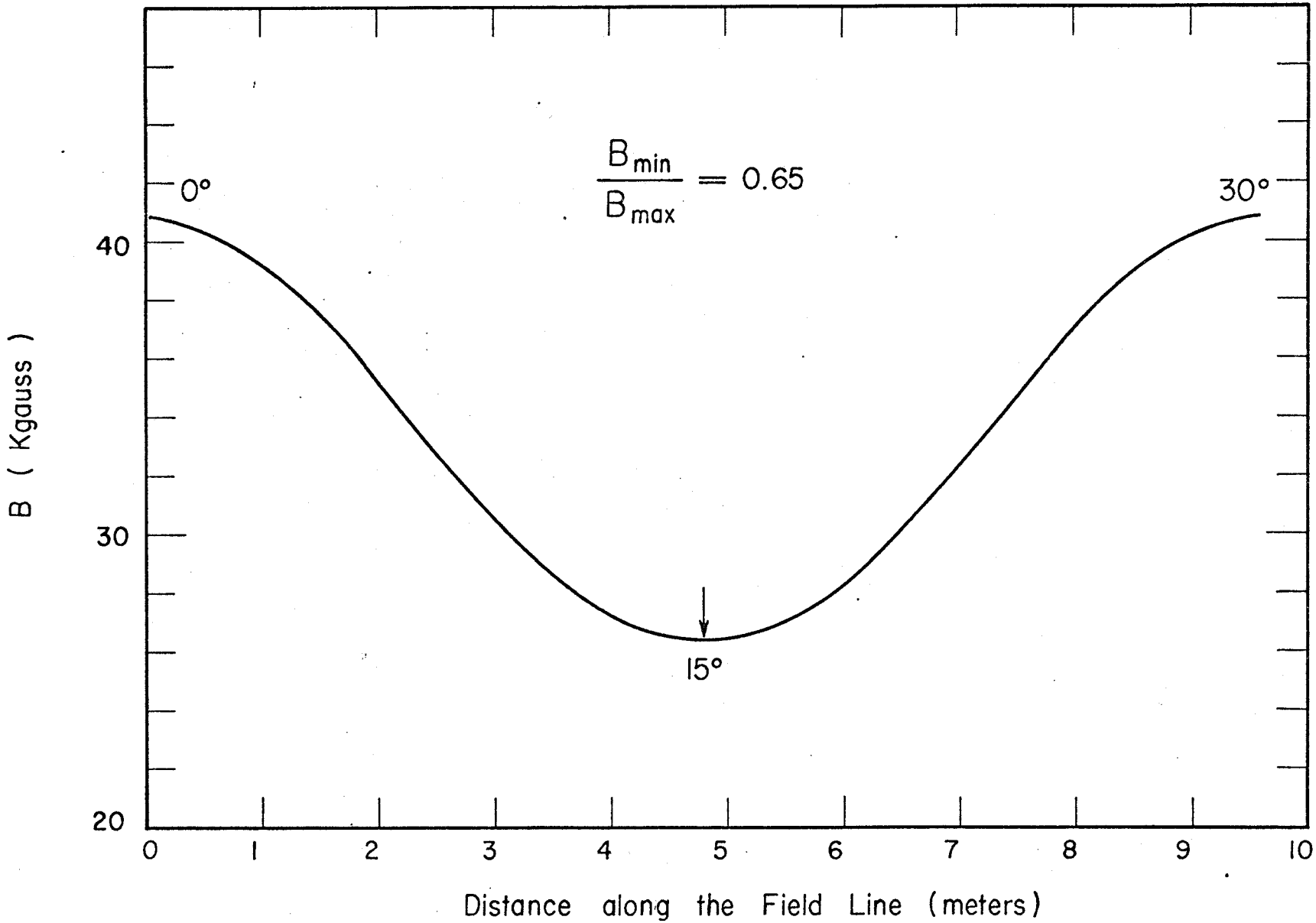

FIGURE 6
Field Variation Along Outer Edge of Plasma at Midplane